DIGITAL GREY BOX MODEL OF THE UNI-VIBE EFFECTS PEDAL

Champ Darabundit *

University of Southern California
Los Angeles, CA
darabund@usc.edu

Russell Wedelich

Eventide Inc.
Little Ferry, NJ
rwedelich@eventide.com

Pete Bischoff

Eventide Inc.
Little Ferry, NJ
pbischoff@eventide.com

ABSTRACT

This paper presents a digital grey box model of a late 1960s era Shin-ei Uni-Vibe®[1] analog effects foot pedal. As an early phase shifter, it achieved wide success in popular music as a unique musical effect, noteworthy for its pulsating and throbbing modulation sounds. The Uni-Vibe is an early series all-pass phaser effect, where each first-order section is a discrete component phase splitter (no operational amplifiers). The dynamic sweeping movement of the effect arises from a single LFO-driven incandescent lamp opto-coupled to the light dependent resistors (LDRs) of each stage. The proposed method combines digital circuit models with measured LDR characteristics for the four phase shift stages of an original Uni-Vibe unit, resulting in an efficient emulation that preserves the character of the Uni-Vibe. In modeling this iconic effect, we also aim to offer some historical and technical insight into the exact nature of its unique sound.

1. INTRODUCTION

The Uni-Vibe was a Shin-ei Companion effects box branded as the Univox Uni-Vibe and distributed by the Unicord Corporation in the late 1960s. The Uni-Vibe is thought to be the prominent guitar effect in popular music recordings such as Jimi Hendrix's Woodstock performance in 1969, Robin Trower's 1974 "Bridge of Sighs," and Pink Floyd's 1973 "Breathe." The sound of the Uni-Vibe is characterized by throbbing pulse, "double beat," and a lo-fi sweep [1]. It has a simple user interface with potentiometer controls for Volume and Intensity, a foot pedal for varying rate or speed, and a switch for Chorus or Vibrato Mode.

While the Uni-Vibe was marketed as a simulation of a rotating "Leslie" style speaker cabinet [2], in a more recent interview the inventor, Fumio Saeda, revealed his inspiration drew more from Radio Moscow broadcasts modulated and distorted by the ionosphere as he listened on short wave radio in Japan [3]. In fact, the Uni-Vibe modulation circuit was largely extracted from his first effects box, the Psychedelic Machine, which was a combination of fuzz and modulation (called Mood), both of which were directly inspired by the combination of fuzzy distortions and pitch modulation of the ionosphere distorted broadcasts.

The Uni-Vibe is considered to be a phaser or phase shifter similar to the MXR Phase 90 of the time [4]. A phaser mixes an input signal with the same signal's output from a series chain of all-pass filters to generate a number of notches in the frequency spectra.

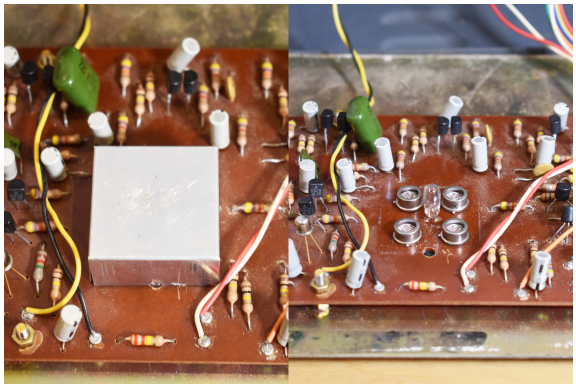

Figure 1: *A closeup of the reflective housing (left) and lamp-LDR assembly (right)*

Each pair of single order all-passes, when mixed with the original signal, creates an instantaneous frequency notch where their 180° phase shifts intersect. For this reason, most phasers match the center frequencies in pairs or use 2nd order filters. Notch locations are modulated by a Low Frequency Oscillator (LFO) sweeping the all-pass center frequencies. As a phaser, the Uni-Vibe is particularly unique in two respects: the instantaneous positions of the notches are determined by the complex interaction between a single incandescent lamp and four adjacent LDRs housed in a roughly cube-shaped reflective chamber (shown in Figure 1), and an almost arbitrary choice of phasing capacitor values. The capacitor values, which determine the all-pass center frequencies, result in staggered or spread notches unlike other phasers which tend to use matched pairs. In addition to a phasing sound this leads to a band limited tremolo-like effect. The exact reasoning for the capacitor selection remains a mystery to Uni-Vibe aficionados [4].

The uniqueness of the Uni-Vibe has thus been the subject of many attempts to commercially clone the original such as ([5] [6] [7]) and [8] by Dunlop Manufacturing who now own the Uni-Vibe trademark, among others. Many of these clones attempt to emulate the Uni-Vibe by recreating the original circuit, or by attempting to replicate a similar lamp and LDR combination.

Previous published work on Uni-Vibe analysis was done in [9] and [10]. Related work in [11] provides a thorough overview for direct digital implementation of generalized analog phasers constructed with operational transconductance amplifiers and field effect transistors. Whereas, the more specific modeling of the MXR Phase 90 pedal from [12] tabulates the main nonlinearity from a JFET used as the notch sweeping variable resistor within a state space discrete model of the circuit. The authors in [13] describe an ad-hoc method for modeling a vactrol, a single element package combining an LED and LDR, in a Buchla low-pass gate. They

* For Eventide Inc.

[1] Uni-Vibe is a registered trademark of Dunlop Manufacturing, Inc.

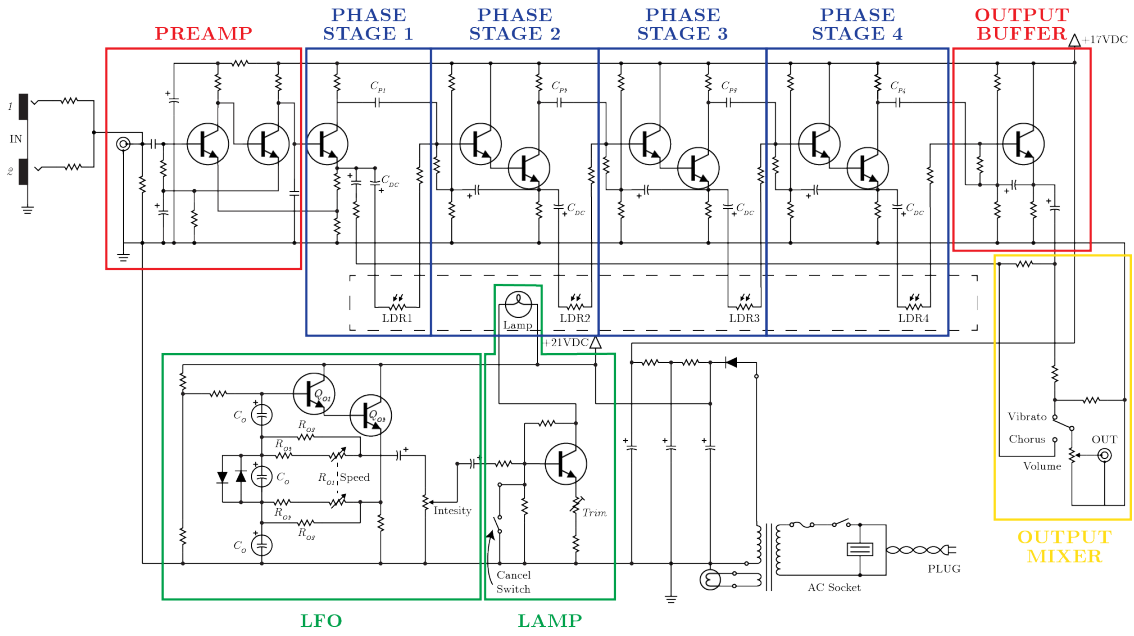

Figure 2: *The complete Uni-Vibe circuit schematic*

reason that realizing full models of photoconductor transients for musical signals is a significant task based on the models in [14].

We propose a digital grey box emulation of the Uni-Vibe, similar to the phaser modeling work done in [15]. The grey box model approach combines physical measurement data (a black box model) and a physically informed model derived from circuit analysis (a white box model). Our primary motivation for this approach, over complete physical modeling of the entire system, arises from the observed complexity in the coupled interaction between the driving LFO circuit, the single incandescent lamp, the four adjacent LDRs, and the reflective housing encasing the lamp and LDRs. We reason that a full model would need to take into account the complex physical relationship of at least the lamp, the LDRs, and the additional reflections and shielding provided by the housing. Since our goal is real-time and efficient implementation of this model, we opted for the black-box approach to this complex system. Consequently, our emulation uses measurement data taken directly from an original Uni-Vibe unit to create three-dimensional wavetables capturing the behavior of each of the LDRs under the influence of the LFO driven incandescent lamp.

While the behavior of the LFO and LDRs is complex, a model of the phasing sections can be derived and discretized via the bilinear transform for the white box portion. Additionally, we will show that the discrete transistor phase splitting does not result in ideal all-passing, and that this does have a perceivable effect in the Uni-Vibe's sound.

This paper will first provide an overview of the Uni-Vibe pedal and circuit in Section 2. In Section 3 we will examine the phasing circuit and the derivation of its continuous-time and discrete-time models, highlighting some of the perceptually relevant aspects yet to be thoroughly covered in previous works. Section 4 will cover the measurement procedure for evaluating the LDRs and the signal analysis done to extract resistance curves from the LDRs. Section 5 will discuss the results and real-time implementation of the preamplifier model of the Uni-Vibe. Section 6 offers conclusions and suggestions for future work.

2. UNI-VIBE CIRCUIT

The Uni-Vibe can be broken down into five basic blocks (as shown in Figure 2): the pre-amplification section, the phasing section, the LFO and lamp section, the output buffer, and the output mixer. The input signal is buffered by the nonlinearity before being passed to the phasing section which is a multi-stage phaser with four phase stages. Each phase stage has its own unique LDR and phasing capacitor, labeled C_P in Figure 2. The LDR and R_6 combined in series forms the resistor-capacitor pair determining the center frequency of the phase-shift contributed by each section.

After passing through the phasing sections, the signal is passed to the output buffer which is a bipolar junction transistor (BJT) buffer, before being passed to the output mixer. Within the output mixer there is the vibrato/chorus switch, along with the volume control knob. The vibrato/chorus switch switches between two resistive networks to determine whether the signal from the output buffer is passed to the output by itself or mixed evenly with a "dry" signal originating from the first phase stage. The volume control is a potentiometer adjusting the amplitude of the output. In comparison to the phasing section and the LFO, the pre-amplification section and the output buffer section do not modulate the audio path in a significant way at low signal levels and their contributions are ignored in our analysis. The effects of these sections at high signal levels due to distortion remain for future work. Volume and the Chorus/Vibrato switch did not need to be extensively modeled as they can be represented by a multiplication and addition, respectively.

2.1. LFO Section

This section contains the most dominant Uni-Vibe controls, Intensity and Speed, found in the LFO section of Figure 2.The Intensity

knob, which goes from a value of one to nine, with additional minimum and maximum settings, scales the LFO voltage across the bulb, and thus determines the range of the notches' frequencies in the phase-shifted signal.The effect of sweeping over a larger frequency at the same LFO speed is what causes notches to sound "deeper." The Speed, controlled via foot-pedal, determines the rate of the LFO. From toe-to-heel the Speed traverses approximately 0 Hz to 7.6 Hz. The 0 Hz Speed originates from a cancel switch located at the heel of the foot pedal that turns off the lamp and prevents the value of the LDRs from changing.

The LFO is a variation on a phase-shift oscillator [4]. A phase-shift oscillator uses regenerative feedback from an RC network from the base of Q_{O1} to the emitter of Q_{O2} to produce a sinusoidal output. The RC network here is the equivalent resistance of the two R_{O1}, R_{O2}, R_{O3} legs along with the three C_O capacitors. The foot pedal controls the speed by varying the value of the coupled potentiometers R_{O1}, which in turn vary the equivalent resistance of the two resistor legs.

Before the LFO signal is passed to the BJT buffer in the lamp section, its amplitude is modulated via the Intensity potentiometer. As the rate of the LFO is dependent on regenerative feedback, coupling the Intensity pot directly to the output of the LFO results in rate drifting proportionally with intensity and vice-versa, resulting in a non-orthogonal relationship between Speed and Intensity. In order to accurately model this parameter interdependency, our black box model utilizes a three-dimensional wavetable, with input phase/sample, speed, and intensity axes.

2.2. Lamp and LDRs

The lamp section of the Uni-Vibe is rather straightforward and consists of a BJT buffer which supplies the LFO signal to the lamp. Within this section is the cancel switch and a trim pot which was not adjusted during our measurements. When the cancel switch is flipped all power to the bulb is cut. The resistance of an LDR is inversely proportional to brightness therefore in complete darkness an LDR is at its maximum resistance. As the center frequency of the phase shifter is inversely proportional to the resistance of the LDR, the cancel switch causes the center frequencies to trend to DC. The cancel switch thus effectively acts as a bypass.

The lamp and the LDRs were specially sourced for the Uni-Vibe. The lamp is a fast-switching incandescent bulb (but not as fast as an LED) and the LDRs are made with cadmium sulfide and are no longer mass produced [3]. The uniqueness and rarity of these components is what, in part, is responsible for the unique tone of the Uni-Vibe.

3. PHASING CIRCUIT ANALYSIS AND MODEL

Figure 3 shows the schematic for phase stages 2, 3, and 4 of the phasing circuit. Each stage consists of a Darlington emitter follower that directly drives a phase inverter whose center frequency is determined by an LDR and phasing capacitor pair, labeled LDR and C_p, respectively. Due to the nature of the Darlington amplifier circuit and C_1 acting as a "bootstrap" capacitor the input impedance of each stage is very high [4]. This allows us to consider each phase stage individually, instead of as a whole. Although phase stage 1 is not driven by a Darlington amplifier, we assume similar behavior as the other phase stages because of the preamplifier section . A similar analysis of this circuit has been done by [9], who modeled the response of each phase stage as

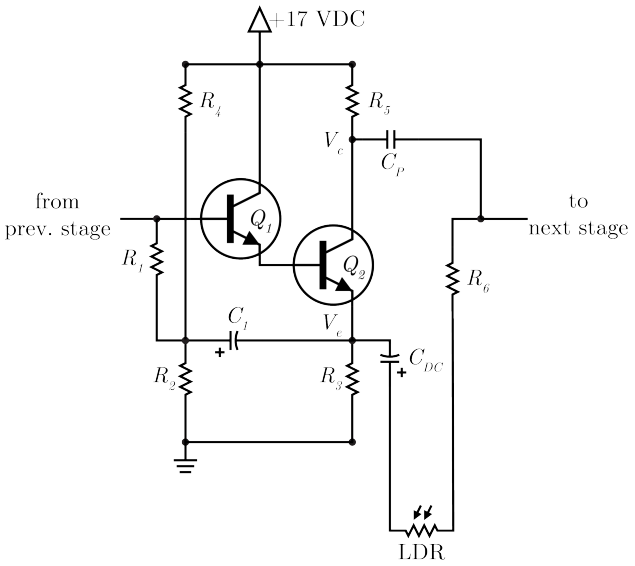

Figure 3: *A single stage of the phasing circuit. The inverting side comes comes off the collector and the non-inverting side comes off the emitter*

an all-pass phaser by representing the Darlington emitter-follower as an phase inverter with gain ≈ 1 feeding an RC bridge. This conclusion assumes, incorrectly, that the amplitude of inverting and non-inverting legs of the transistor originating from the collector and emitter of Q_2 are balanced, and that the block capacitor's (C_{DC}) contribution can be ignored. Through listening, measurement, and simulation of the Uni-Vibe it was determined that these factors could not be ignored and had to be taken into account, thus a corrected analysis of the circuit is presented below.

3.1. Phasing Circuit Analysis

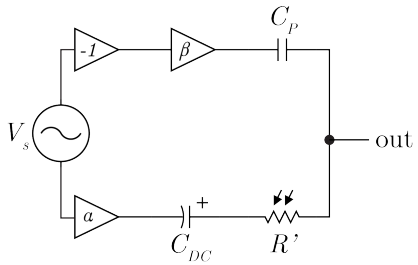

Figure 4: *A block diagram describing the corrected phasing circuit.* $R' = \text{LDR} + R_6$

Figure 4 represents the incoming signal to each stage as V_s, the phase inversion as a gain of -1, and the inverting and non-inverting gains as β and α, respectively. The phasing capacitor and the block capacitor remain unchanged while the value R' represents the series resistance of the LDR and R_6.

The transfer function $H(\omega)$ of the phasing circuit can be found through the superposition of two complex voltage dividers taken from the inverting and non-inverting legs of the circuit. Analyzing the phasing circuit in this manner makes a digital implementation

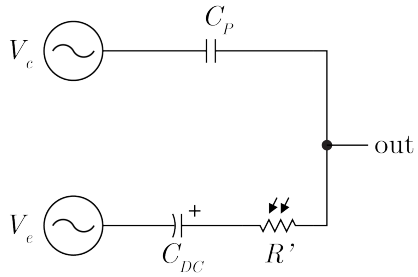

Figure 5: *A further simplification of the phasing block diagram where the V_s, α, and β have been simplified as an inverting and non-inverting source*

of the filter and application of nonlinearity easier as will be shown in Sec. 3.2. This simplification is represented in Figure 5, where:

$$V_e = \alpha V_s \tag{1}$$

and,

$$V_c = -\beta V_s \tag{2}$$

Giving us the complete transfer function:

$$H(\omega) = H_c(\omega) + H_e(\omega) \tag{3}$$

$H_c(\omega)$ and $H_e(\omega)$ are the transfer functions of the inverting and non-inverting legs:

$$H_c(\omega) = \frac{\kappa_c \omega_o + j\omega}{\omega_o + j\omega} \tag{4}$$

$$H_e(\omega) = \frac{\kappa_e \omega_o}{\omega_o + j\omega} \tag{5}$$

Where:

$$\kappa_c = \frac{C_p}{C_p + C_{DC}} \tag{6}$$

$$\kappa_e = \frac{C_{DC}}{C_p + C_{DC}} \tag{7}$$

are constants, and

$$\omega_o = \frac{1}{R'} \frac{C_{DC} + C_p}{C_p C_{DC}} \tag{8}$$

is the center frequency of the filter. If we combine equations (1) (2) (3) (4) (5) we have the transfer function of the entire phasing circuit:

$$H(\omega) = \alpha \left(\frac{\kappa_e \omega_o}{\omega_o + j\omega} \right) - \beta \left(\frac{\kappa_c \omega_o + j\omega}{\omega_o + j\omega} \right) \tag{9}$$

Which has the phase response:

$$\phi(\omega) = \tan^{-1} \left(\frac{-\beta\omega}{\alpha\kappa_e\omega_o - \beta\kappa_c\omega_o} \right) - \tan^{-1} \left(\frac{\omega}{\omega_o} \right) \tag{10}$$

If we let $\beta = 1$, $\alpha = 1$ (i.e. the inverting and non-inverting gains are balanced) and $C_{DC} = \infty$ (which removes the effect of the block-capactior) equation (9) takes the form of a standard first-order all-pass phaser in equation (11), as $\kappa_c = 0$, and $\kappa_e = 1$.

$$H(\omega) = \frac{\omega_o - j\omega}{\omega_o + j\omega} \tag{11}$$

Which matches the analysis done by [9]. If the same equalities are applied to equation (10) we obtain the standard phase response of a first-order all pass:

$$\phi(\omega) = -2\tan^{-1} \left(\frac{\omega}{\omega_o} \right) \tag{12}$$

Since the bootstrap capacitor C_1 allows us to assume high input impedance at each stage the full cascade of the phasing section is:

$$H(\omega) = \prod_{n=1}^{4} H_{c_n}(\omega) + H_{e_n}(\omega) \tag{13}$$

Where,

$$H_{c_n}(\omega) = \frac{\kappa_{c_n}\omega_{o_n} + j\omega}{\omega_{o_n} + j\omega} \tag{14}$$

$$H_{e_n}(\omega) = \frac{\kappa_{e_n}\omega_{o_n}}{\omega_{o_n} + j\omega} \tag{15}$$

and,

$$\kappa_{c_n} = \frac{C_{p_n}}{C_{p_n} + C_{DC}} \tag{16}$$

$$\kappa_{e_n} = \frac{C_{DC}}{C_{p_n} + C_{DC}} \tag{17}$$

$$\omega_{on} = \frac{1}{R'_n} \frac{C_{DC} + C_{p_n}}{C_{p_n} C_{DC}} \tag{18}$$

for each phase-stage ($n = 1, 2, 3, 4$).

Table 1: *Measured capacitance, inverting, and non-inverting gains, and LDR resistances*

	C_p (*F*)	α	β	LDR (Ω)		
				avg (M)	*min. (k)*	*max. (M)*
1	.015μ	1.01	1.11	0.405	12.7	2.79
2	.22μ	.98	1.09	0.233	6.86	2.59
3	470p	.97	1.10	0.29	7.69	3.32
2	.0047μ	.95	1.09	0.240	6.22	4.16

Each stage has its own unique H_{c_n}, H_{e_n}, κ_{c_n}, κ_{e_n}, and ω_{on} as each stage has a unique phasing capacitor, LDR, inverting gain, and non-inverting gain which were found through measurement of each phase stage. Table 1 provides these values. We should note that these values are most likely unique to the particular unit we measured, and we expect these values are varied among differing Uni-Vibe units given the tolerances of the components. Different units most likely have their own particular sound.

The inclusion of the inverting and non-inverting gains as well as the block capacitor in the analysis of the phasing circuit are a sonically relevant addition to the analysis and modeling of the Uni-Vibe. As seen in Figure 6 with R' fixed at LDR1's mean value the block capacitor causes the magnitude of the transfer function to exhibit a high shelf response rather a unity response all-pass filter. This high shelf effect is emphasized as the stages stack up. Additionally dissimilar inverting and non-inverting gains, along with the block capacitor cause a shift in the phase response of the filter as seen in equation (10). In chorus mode the sweeping high shelf causes the low end of the signal to match what the output

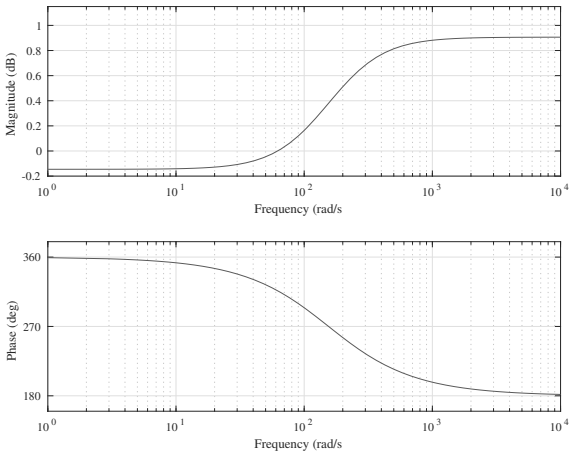

Figure 6: *Transfer function of the first phase stage.* $\alpha = 1.0009$, $\beta = 1.11$, $R' = 409.7\text{k}\Omega$

would be in vibrato mode and is responsible for the Uni-Vibe's characteristic throbbing pulse.

We reason that the selection of the phasing capacitor values is such that only two notches can heard at a time, which creates the Uni-Vibe's characteristic double beat. As the Uni-Vibe stages are not matched pairs like other phasers, without the inclusion of the block capacitor instantaneous notches can "pop" in and out of the frequency spectra.

3.2. Discrete Model

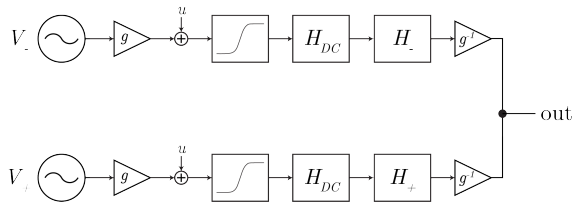

Figure 7: *Block diagram of the applied nonlinearity*

From equations (14) (15) a discrete model of each phase stage circuit was derived using the bilinear transform and pre-warping the filter around the frequency ω_{on} giving us the discrete transfer functions for the inverting and non-inverting legs:

$$H_{c_n}[z] = \frac{(\kappa_{c_n}\text{tan}\omega_{o_n} + 1) + (\kappa_{c_n}\text{tan}\omega_{o_n} - 1)z^{-1}}{(\text{tan}\omega_{o_n} + 1) + (\text{tan}\omega_{o_n} - 1)z^{-1}} \tag{19}$$

$$H_{e_n}[z] = \frac{\kappa_{e_n}(1 + z^{-1})}{(\text{tan}\omega_{o_n} + 1) + (\text{tan}\omega_{o_n} - 1)z^{-1}} \tag{20}$$

in the complete discrete equation:

$$H_n[z] = H_{c_n}[z] + H_{e_n}[z] \tag{21}$$

for each stage $(n = 1, 2, 3, 4)$.

It is important to note that ω_{on} is dependent on the value of the LDR and therefore the bilinear transform and frequency pre-warping must be applied in real-time.

3.2.1. Non-linear elements

It was determined through measurements that the emitter-follower pair in each phase-stage was clipping the input signal asymmetrically. To approximate this non-linear behavior, a tanh() function with a heuristically determined bias and scaling factor is applied in the signal chain before (21). Separating our signal into two signal paths allows us to apply this nonlinearity. A block-diagram of how this nonlinearity is incorporated is shown in Figure 7. Including these non-linearities was necessary in modeling the Uni-Vibe as the clipping added audible harmonics and the biasing adjusted the balance of even and odd harmonics.

The scaling factor g determines the level at which the signal clips by gaining down the input signal. The biasing factor u offsets the signal to determine the extent of the asymmetry in the clipping. The ideal values for g and u were first determined through measurement of the original Uni-Vibe pedal, and then tuned heuristically to match. After the signal is clipped by the tanh() function it is passed through a DC-blocking low-pass filter. The inclusion of this filter is an improvement on the original signal path of the Uni-Vibe. The biasing factor u, which exists in both the Uni-Vibe and in our model, pushes DC impulses through to the output when ω_o approaches DC. These impulses are audible as clicking in the original Uni-Vibe. Our DC-blocking filter removes the DC offset before equation (19) (20) are applied. Before being outputted the signal is gained back up by g^{-1} to return the signal level back to its original value. The gain values are fairly low, so aliasing distortion due to clipping is also fairly minimal, thus in order to keep the model efficient we neglected any oversampling.

4. MEASURING THE UNI-VIBE LDRS

4.1. Physical Measurement

Due to the difficulty in physically modeling the transient resistance of the LDRs in the phase stage, a decision was made to measure the behavior instead. Unlike [10] which measures a Uni-Vibe clone, we directly measure the actual Uni-Vibe unit. Additionally [10] only measures one LDR, while we found it important to measure all four as we could not ensure the LDRs would have the same values based on their make and position respective to the lamp. This decision is supported by Table 1 which demonstrates that each LDR differed from one another. To measure the behavior of a phase stage's LDR the output of the stage was shorted and the input was fed with a 1 kHz sine wave. Voltage measurements were taken across the LDR and R_6 and across R_6 alone, allowing us to derive the transient resistance of the LDR as part of a voltage divider.

$$R_{\text{LDR}} = R_6 \frac{V_{\text{LDR}}}{V_6} - R_6 \tag{22}$$

Measurement recordings were taken by playing the 1 kHz input signal while in tandem taking the two aforementioned voltage measurements. These measurements were recorded on a digital audio workstation using the Expert Sleepers ES-8 USB-audio interface which has DC-coupled inputs and outputs [16]. To model the full breadth of the pedal these measurements were repeated at fourteen different LFO frequencies and at eleven different intensities settings for each of the four LDRs. Consequently an additional measurement was taken of the LFO signal driving the lamp, as a method of recording the speed of the LFO in the case of any inconsistencies in the foot pedal settings during measurement.

4.2. Measurement Analysis

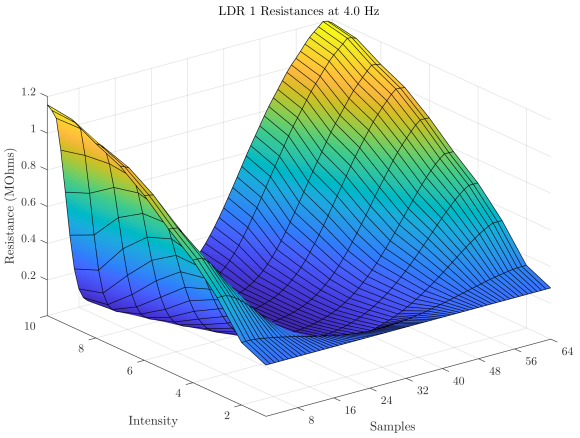

Figure 8: *A complete wavetable for LDR1 at 4 Hz*

The process taken to analyze the measurement for each LDR were as follows. The measurement data was converted to their nominal RMS values based on the specifications of the USB-audio interface. The recordings were then upsampled by four so envelope extraction could be performed using a maximum value filter with a rectangular window with a width of 1 kHz. This allowed us to extract the effect of the circuitry and remove the 1 kHz input signal. Additional filtering was also done to remove power-supply hum. A model of the additive noise in the LDR resistances was found by deriving the transient resistance of an LDR using equation (22) at a minimum Intensity for each Speed. This noise model could then be used in conjunction with a Wiener filter, using Matlab's `wiener` function, to remove any noise in transient resistances at higher Intensity settings.

At this point, single-cycle resistance curves needed to be extracted from the clean resistance signal. To preserve more perceptible information single-cycle curves were extracted by using local maximums to determine the starting and ending peaks for individual periods in the resistance signal. Unfortunately information is lost at the loop point from the start to the end of a cycle. To minimize this local maximums were chosen as the loop point because ω_o values arising from the resistances at local minimums are much more perceptible than ω_o values arising from the local maximums, which approach DC. Each single-cycle period was averaged together to further reduce noise in the resistance signal.

To prepare these resistance curves for implementation in the wavetable each one-period length curve was then downsampled to 64-samples. Then, using the LFO rate data obtained from an FFT of the LFO signal, curves of a similar Intensity were interpolated to be equally spaced across the entire frequency range of the LFO. This was done to facilitate indexing across the lookup table. The first two-samples and last two-samples of each curve were interpolated together to ensure that the loop point was seamless at the expense of data loss. Otherwise, any significant disjoint would be perceived as an audible click. The result of this analysis is a three-dimensional wavetable containing 640 unique LDR resistance curves for each LDR representing every combination of Speed and Intensity settings on the Uni-Vibe, with a sawtooth phase input providing exact sample accurate rate. Figure 8 shows a small sample of this wavetable containing the curves for the first LDR at a speed of 4 Hz. Visual analysis of the resistance curves shows the curves have increasing asymmetry as intensity increases due to the LDRs having different turn-on and turn-off times. The increasing asymmetry is a result of lamp varying its brightness more rapidly as intensity is increased.

5. RESULTS AND EXPERIMENTS

5.1. Real Time Implementation

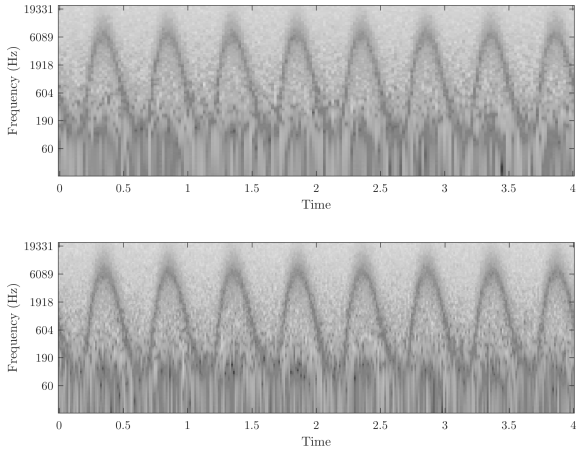

Figure 9: *Noise Spectrograms. Top: Model, Bottom: Uni-Vibe. A second notch can be seen in the lower frequencies under the main notch.*

A real-time implementation of the the Uni-Vibe emulation was implemented in C/C++ both as a VST plugin using the JUCE framework and as a process running in a single core of an embedded Linux ARM Cortex-A9 commercial audio product. The real-time emulation consists of four *univibe_phaser* modules each of which replicates a single stage of the phasing circuit by using the measurement derived three-dimensional wavetable and the discrete-time model of the Uni-Vibe's phase-stage.

Depending on the selection of which stage to emulate the *univibe_phaser* module converts the wavetable of LDR resistances into a wavetable of center frequencies ω_o before implementation using the known values of each stages' C_p and C_{DC}. Using a graphical user interface the desired Intensity and LFO Speed can be set to linearly interpolate a value of ω_o from the wavetable. This value is then passed to an implementation of equation (13).

Figure 9 shows spectrogram output of our real-time implementation and the original Uni-Vibe with white noise as the input source. Upon visual inspection, the model retains the dynamic behavior of the original unit. Intensity and Speed settings were 7 and 2.0 Hz respectively.

5.2. Experimental Methodology

MUSHRA style listening tests were conducted to quantitatively assess the accuracy of our real-time implementation of the Uni-Vibe running in the ARM Cortex-A9 commercial audio product. A second original Shin-ei Uni-Vibe, two analog hardware clones, and two digital emulations in hardware were tested alongside our

implementation for a total of 6 units under test. The original hardware unit measured for our implementation was chosen as the MUSHRA reference.

5.2.1. MUSHRA Test Setup

Reference and MUSHRA anchor recordings were generated as follows: Unaffected electric guitar passages were recorded into a UAD Apollo 8 interface via Direct Injection, or DI. Reference recordings were created by feeding recorded passages through the original Uni-Vibe set at specific Intensity and Speed settings. All recordings were done in Chorus mode with Volume set at 5. Due to the relatively low frequency spectral quality of the electric guitar, 1.5 kHz low-passed versions of the reference recordings were included as anchors instead of the usual 7 kHz and 3.5 kHz low-passed anchors.

For test unit recordings, Intensity settings were visually matched to the reference through printed markings or numerically via graphical displays where applicable. Test unit LFO Speed settings were precisely matched to the reference through waveform inspection of their phase cancellation cycle or numerically via graphical displays where applicable. Trial and error was used to ensure LFO phase alignment between test unit recordings and the reference recording.

5.2.2. Electric Guitar Passage Selection

A total of three electric guitar passages were recorded for the listening tests. Passages were disparately styled and chosen to reflect real-world use cases for the Uni-Vibe in addition to test the full range of Uni-Vibe sounds and settings.

Passage 1 consisted of a 101 BPM Texas Blues styled riff played with hard plectrum attack intended for a Uni-Vibe set to approximate a Leslie in tremolo mode. Reference Intensity and Speed settings were 5 and 4.85 Hz respectively creating a triplet modulation feel.

Passage 2 consisted of a 4 bar phrase using whole note chords followed by an arpeggiated version of the same chord progression played at 110 BPM. Reference Intensity and Speed settings were 7 and 1.89 Hz respectively for a medium depth modulation that followed the quarter note.

Passage 3 consisted of a 62 BPM, two open-chord arpeggiation. Intensity and Speed settings were set at 10 and 0.99 Hz respectively creating a slow and deeply swept modulation. Settings were chosen so participants could best judge LFO modulation contours in the test.

5.3. Experimental Results

Listening tests were administered using webMUSHRA software [17] and a total of 20 participants were included in the test. Figure 10 shows a box plot of the results of listening test 1 where our model scored closest to the reference. Of the analog hardware units tested, scores varied widely with two units averaging below the digital emulations. The second original Uni-Vibe scored substantially lower than the reference which seemed to confirm our initial listening impressions of the high degree of variability between these specific original units. Given the majority of units tested closer to the reference, we suspect the second original Uni-Vibe could be out of factory specification warranting further investigation. Post-test user feedback for listening test 1 revealed a wide range of criteria for judging similarity and included pick

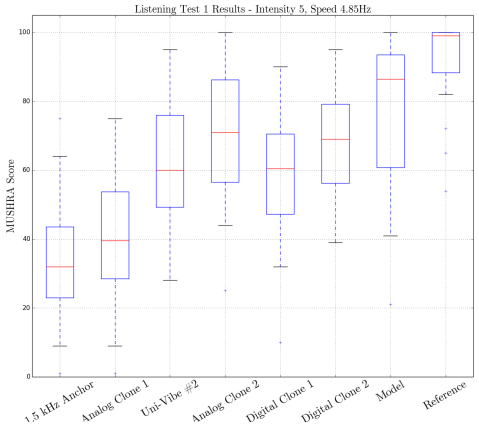

Figure 10: *Listening test 3 results*

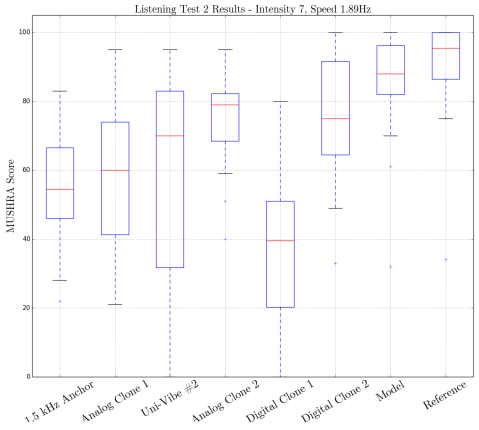

Figure 11: *Listening test 2 results*

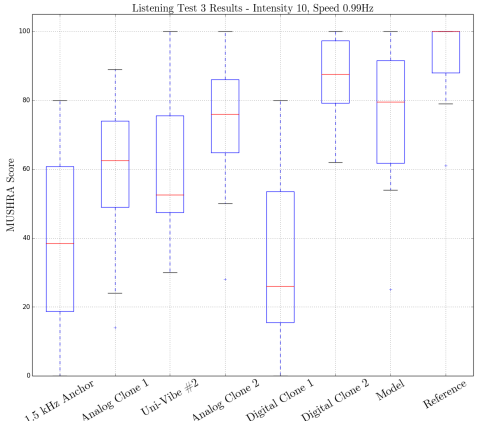

Figure 12: *Listening test 3 results*

attack, tonal balance (timbre), modulation depth, and noise floor. The wide range of judgement criteria may explain the large interquartile sizes and low score outliers in these results.

Figure 11 shows a box plot of the results of listening test 2. These results mirrored listening test 1 however, Digital Clone 1 scored below the anchor. During our own informal comparisons, Digital Clone 1's depth of modulation and overall timbre were markedly different than the reference, both most likely playing large roles when tests were scored by participants. Anchor scores averaged higher than listening test 1 indicating low pass frequency may have been set too high. Post-test user feedback reported listening test 2 as harder to judge than listening test 1 which could explain the average score increase for most units.

Figure 12 shows a box plot of the results from listening test 3. As in test 2, Digital Clone 1 scored lowered than the anchor, most likely for reasons similar to listening test 2. Our model scored second closest to the reference with Digital Clone 2 scoring the highest. Post-test user consensus deemed listening test 3 hardest to score of the three tests. From our own qualitative listening sessions at these settings, our implementation exhibited a slightly deeper and squarer-edged modulation contour than the reference. We believe this is related to our choice of wavetable splice point and interpolation.

6. CONCLUSION

In this work a grey box method was proposed for creation of an accurate Uni-Vibe model. A white-box model of the Uni-Vibe's phasing circuit was created through circuit analysis uncovering aspects of the Uni-Vibe circuit that contribute to its iconic sound. A complementary black-box model was also created through measurement of the Uni-Vibe's LFO-LDR-lamp interaction. A real-time implementation of the grey box model of the Uni-Vibe was implemented on a single core of a Linux ARM Cortex-A9. In comparison to an original unit and other Uni-Vibe clones our implementation was on-average rated closest to the reference in two out of three MUSHRA listening tests, scoring second in the third test.

Further work to improve our model would be deriving and implementing more accurate behavior of the non-linear BJT clipping, as was done by [18], instead of replicating it heuristically. We also plan to further investigate the ideal method of splicing at the wavetable loop point. Conversely, judging from our measurements of the LFO-LDR-lamp interaction, it may be also possible to create a simplified parametric model of that interaction.

7. ACKNOWLEDGMENTS

Special thank you to Chuck Zwicky (www.zmix.net) for making Uni-Vibe recordings of his original unit for the listening test comparisons.

8. REFERENCES

[1] H. Shapiro, M. Heatley, and R. Mayer, *Jimi Hendrix Gear*, Voyageur Press, Minneapolis, MN, USA, 2014.

[2] Unicord Incorporated, *Uni-Vibe Operating Manual*, 1968.

[3] M. Yoshiyuki, "What is Uni-Vibe? pt.1," `https://www.digimart.net/magazine/article/2018052303189.html`, May 5 2018.

[4] R. G. Keen, "The technology of the univibe," `http://www.geofex.com`, accessed March 5, 2019.

[5] MJM Guitar FX, "Sixties Vibe Classic," `http://mjmguitarfx.com/product/sixties-vibe-classic/`, accessed March 5, 2019.

[6] Black Cat Pedals, "Black Cat Vibe," `http://www.blackcatpedals.com/black-cat-vibe/`, accessed March 5, 2019.

[7] Fulltone, "Mini Dejavibe 3 V2," `https://www.fulltone.com/products/mini-dejavibe-3-v2`, accessed March 05, 2019.

[8] Dunlop Manufacturing Inc., "Univibe Chorus/Vibrator," `https://www.jimdunlop.com/product/m68-7-10137-07227-5.do`, accessed March 05, 2019.

[9] C. Hahlweg and H. Rothe, "The unique sound of the Uni-Vibe pedal," in *Proc. SPIE 8487, Novel Optical Systems Design and Optimization XV*, San Diego, California, United States, Oct. 19 2012.

[10] C. Hahlweg and H. Rothe, "The unique sound of the Uni-Vibe pedal: Part ii. transient behaviour," in *Proc. SPIE 8842, Novel Optical Systems Design and Optimization XVI2*, San Diego, California, United States, Sept. 30 2013, pp. 1–8.

[11] A. Huovilainen, "Enhanced digital models for analog modulation effects," in *Proc. Digital Audio Effects (DAFx-05)*, Madrid, Spain, Sept. 20–22, 2005, pp. 155–160.

[12] F. Eichas, M. Fink, M. Holters, and U. Zölzer, "Physical modeling of the MXR phase 90 guitar effect pedal," in *Proc. Digital Audio Effects (DAFx-14)*, Erlangen, Germany, Sept. 1–5, 2014, pp. 153–158.

[13] J. Parker and S. D'Angelo, "A digital model of the buchla lowpass gate," in *Proc. Digital Audio Effects (DAFx-13)*, Maynooth, Ireland, Sept. 2–6, 2013, pp. 278–285.

[14] A. E. Iverson and D. L. Smith, "Mathematical modeling of photoconductor transient response," *IEEE Trans. on Electron Devices*, vol. 34, no. 10, pp. 2098–2107, 1987.

[15] R. Kiiski, F. Esqueda, and V. Välimäki, "Time variant grey-box modeling of a phaser pedal," in *Proc. Digital Audio Effects (DAFx-16)*, Brno, Czech Republic, Sept. 5–9, 2016, pp. 31–38.

[16] Expert Sleepers Ltd., "ES-8 USB Audio Interface," `https://www.expert-sleepers.co.uk/es8.html`, accessed June 19, 2019.

[17] Michael Schoeffler, Sarah Bartoschek, Fabian-Robert Stöter, Marlene Roess, Susanne Westphal, Bernd Edler, and Jürgen Herre, "webMUSHRA: a comprehensive framework for web-based listening tests," *Journal of Open Research Software*, vol. 6, no. 1, 2018.

[18] D. T. Yeh, "Automated physical modeling of nonlinear audio circuits for real-time audio effects - part ii: BJT and vacuum tube examples," *IEEE Trans. on Speech and Audio Processing*, vol. 18, no. 3, pp. 1207–1216, 2011.